Volume - 11 | Issue - 09 | September - 2022 | PRINT ISSN No. 2277 - 8179 | DOI : 10.36106/ijsr

INTERNATIONAL JOURNAL OF SCIENTIFIC RESEARCH

RADIATION PROTECTION PURPOSES IN DIAGNOSTIC X-RAYS UNITS USING SIMPLE OR COMMON BUILDING MATERIALS

Medical Physics

Ioannis Vlachos	Department of Medical Physics, School of Medicine, University of Patras, Patras 26500, Greece.
Nektarios Kalyvas	Department of Biomedical Engineering, University of West Attica, Athens 12243, Greece.
Gerasimos Messaris	Department of Radiology, University Hospital of Patras, Patra 26504, Greece.
George Fountos	Department of Biomedical Engineering, University of West Attica, Athens 12243, Greece.
Harry Delis	Department of Medical Physics, School of Medicine, University of Patras, Patras 26500, Greece.
Ioannis Kandarakis	Department of Biomedical Engineering, University of West Attica, Athens 12243, Greece.
George Panayiotakis*	Department of Medical Physics, School of Medicine, University of Patras, Patras 26500, Greece. *Corresponding Author

ABSTRACT

Diagnostic and interventional radiology is an essential part of present-day medical practice. Advances in X-ray imaging technology, together with developments in digital imaging, have had a significant impact on the practice of radiology. Although individual doses associated with conventional radiography are usually low, examinations involving computed tomography and international radiography can be significantly higher. However, with well-designed, installed, and maintained X-ray equipment, and through the use of proper procedures by trained operators, unnecessary exposure to patients can be reduced significantly, with no degradation in the medical information derived. In all facilities and for all equipment types, procedures must be in place in order to ensure that exposures to patients, staff and the public are kept as low as reasonably achievable. In this work, a more detailed experimental investigation of the scatter X-ray attenuation properties of common building materials such as single ceramic tile, reinforced ceramic tile, double reinforced ceramic tile, glass block, single plasterboard (or gypsum board wall), double plasterboard, was performed.

KEYWORDS

INTRODUCTION

X-ray use in Medicine and other practices was currently addressed through directives [1,2], whose primary focus is the protection of the patients, the radiation workers, and the public. The latter is achieved through establishing dose levels or limits that should not be exceeded, during any well designed practice [1, 2]. To achieve these limits, shielding of areas adjacent to the X-ray tube is necessary. The primary material for shielding for energies used in radiography is lead, while at lower energies like X-ray mammography, other materials like gypsum or brick could suffice [3, 4, 5]. Methods and protocols considering the current X-ray imaging applications have been published [3-8] to calculate the optimum shield thickness of lead or other materials. A conservative approach is to consider an upper X-ray tube voltage of 100kV and calculate the required shield thickness. There are cases, however, that the used X-ray energy is systematically below the 100 kVp X-ray spectra considered in radiographic applications. In veterinary practices, for instance, the range of radiographic energies is between 48 kV to 115 kV, where the larger energies are mainly for equine imaging or large canine thorax examinations [9-11]. Also, in dental X-ray imaging, the simple dental X-ray units operate between 60 kVp-70 kVp, while in Cone Beam Computed Tomography (CBCT) and panoramic imaging several vendors using the energy of 70 kVp [12-19]. In these cases, more straightforward and common materials like glass-block, gypsum, and tile may prove of interest as radiation buriers [5, 20, 21]. The aim of this work is the experimental investigation of such materials for radiation protection purposes. The investigation considers direct exposure measurements, as well as X-ray spectra measurements of the scatter radiation.

Previous work in secondary radiation measurement has considered radiation mapping from radiographic X-ray systems [15, 22, 23] and spectra measurements of X-rays penetrating low atomic number, Z, materials for narrow shaped X-ray fields [15, 20-23]. In this work, a more detailed experimental investigation of the scatter X-ray attenuation properties of common building materials such as single ceramic tile, reinforced ceramic tile, double reinforced ceramic tile, glass block, single plasterboard (or gypsum board wall), double plasterboard, was performed. In addition, higher Z materials such as brazen, iron, steel, lead, zinc, and copper were also investigated. The investigation involved two X-ray fields of 70 kVp tube voltage (7.5x7.5 cm2, and 16x2 cm2), for the standard building materials, as well as measurements at 100kVp with an X-ray field of 40x40 cm2, for the higher Z materials. The measurements incorporated X-ray energy transmission spectra from the materials as well as Air Kerma attenuation properties. The presented measurements allowed the determination of a practical broad beam X-ray transmission efficiency of the materials as well as the determination of their average energy. Our results may be of importance in the calculation of X-ray protective barriers for specific dental X-ray applications or veterinary X-ray installations for small size pets.

MATERIALS AND METHODS

Experimental Setup

A conventional radiographic system Philips Optimus 80, installed at the Radiology Department of the Sismanoglio General Hospital of Athens, Greece, was used to measure the secondary X-ray spectra. The system HVL was measured 2.1 mmAl at 70 kVp.

In order to simulate the human head, a cylindrical phantom from Plexiglas with a diameter of 16 cm and a height of 15 cm was used. The simple symmetrical shape of the phantom diminished the effect of the phantom shape to the measured scattered radiation [23, 24]. The phantom was placed on the radiographic table, and the distance between the phantom and the focal spot of the tube was 83 cm. The distance between the central point of the phantom and the point of measurement of the secondary radiation was fixed at 50 cm [20].

An Amptek XR-100 CdTe spectrometer, with a 2 mm collimator, was used for measuring secondary X-rays energy distribution; that is the scatter X-ray spectrum. [14, 15, 20, 21, 25, 26]. In X-ray spectrum

 PRINT ISSN No. 2277 - 8179 | DOI : 10.36106/ijsr

measurements, the tube voltage was stable at 70 kVp, the tube load was stable at 50 mAs, and the irradiation time was automatically set at 160 ms. The response of the spectrometer for various energies in terms of energy per bin and detector quantum efficiency per energy value were known through calibration in various radiation energies and published literature [26, 27]. In more detail, the correction of the spectrometer concerning the energy, E, per X-ray bin was equal to (1/5.89) keV. In each energy bin, N(E) counts were measured by the spectrometer corresponding in an X-ray spectral energy E. The detected counts were corrected by dividing N(E) with the quantum efficiency response, QER (E), of CdTe which was obtained from the manufacturer data sheet [23, 26, 27]. Therefore the corrected counts per energy bin, f(E), were found as :

$$f(E)=N(E)Q(E) \qquad (1)$$

where

Q(E)=1/(QER(E))= 0.000002*E^3-0.0001*E^2+ 0.008*E+1.0362 (2)

The average measured energy, Eav was calculated according to the following formula.

$$E_{av}=\frac{\sum_{E} Ef(E)}{\sum_{E} f(E)} \qquad (3)$$

In order to measure the dose rate (mSv/hr), a calibrated ionization chamber, 451P-DE-SI model of Fluke Biomedical, was used [28]. In dose rate measurements, the irradiation time was kept constant at 2000 ms, to account for the response time of 451P-DE-SI [29].

The materials which were studied as potential barriers for the secondary X-ray transmission were: a) Single ceramic tile with thickness at 0.7 cm, b) reinforced ceramic tile with thickness at 0.8 cm, c) double reinforced ceramic tile with thickness at 1.8 cm, d) glass block with thickness at 7.9 cm, e) single plasterboard (or gypsum board wall) with thickness at 1.3 cm f) double plasterboard with thickness at 2.6 cm. g) brazen with thickness at 1.0 mm, h) iron with thickness at 1.0 mm, g) steel with thickness at 1.0 mm, i) lead with thickness at 1.0 mm, j) zinc with thickness at 1.0 mm, k) Copper with thickness at 1.0 mm and l) aluminium with thickness at 2.0 cm. All thicknesses were measured with a vernier calliper with reading error 0.05 mm.

For materials (a) to (f), the irradiation conditions were fixed at 70 kVp. The chosen irradiation fields were at 7.5 cm x 7.5 cm and 16 cm x 2 cm, to simulate current dental and veterinary practices. The measuring errors of the procedure are described in the literature [23].

For materials (g) to (l) only spectra, measurements in higher irradiation conditions were performed. In particular, the X-ray tube voltage was at 100 kVp, and the irradiation field was at 40.0 cm x 40.0 cm.

The radioprotection properties of each material were accessed by measuring the X-ray dose rate before (mSv/h)b and after inserting the material (mSv/h) a in front of 451P-DE-SI. The percent transmission for each material TkVp was calculated as:

$$T^{xy}_{kVp}=\frac{\left(\frac{mSv}{h}\right)_a}{\left(\frac{mSv}{h}\right)_b}100\% \qquad (4)$$

Where xy are the dimensions of the X-ray field

When the percent transmission of the block is known, a practical number of tenth value layers (TVL) of the block thickness can be calculated as:

$$N_{TVL}=\log\left(\frac{1}{T^{xy}_{kVp}/100}\right) \qquad (5)$$

Where log corresponds to the decimal logarithm and NTVL to the number of TVLS. The calculation of NTVL is useful in determining the total number of material thickness required to achieve an optimum level of radiation protection.

If the total thickness (TT) and NTVL are known as a practical TVL of the material can be calculated as: $TVL=\frac{TT}{N_{TVL}}$

In order to anticipate for X-ray tube differences between various X-ray vendors equipment, a Philips Digital Diagnost radiographic unit which was installed in the Radiological Department of the University General Hospital of Patras Greece, was additionally used to obtain a secondary dose mapping for 7.5 cm x 7.5 cm and 16 cm x 2 cm irradiation fields. The system HVL at 70 kVp was measured at 2.8 mmAl. The measuring was performed with an Unfors EDD-30 multimeter, which incorporates a sensor capable for measuring the secondary radiation dose in μGy [30]. The scatter radiation was measured at different scattering angles around the phantom from plexiglas (0o to 315o, with a step of 45o) and distances of 0.5, 1.0 and 1.5 m respectively from the centre of the phantom, for different irradiation fields and keeping stable the exposure parameters, as demonstrated in Figure 1.

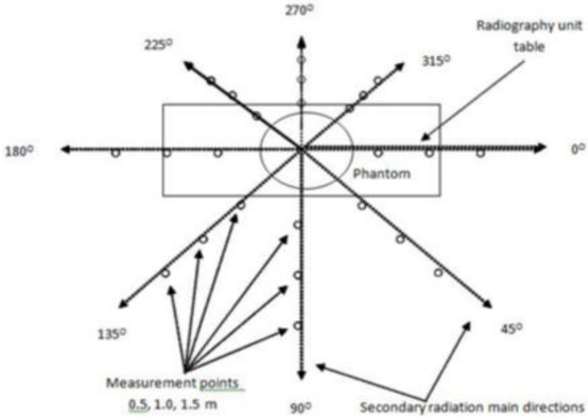

Figure 1. Measurement Setup For Philips Digital Diagnost.

RESULTS AND DISCUSSION

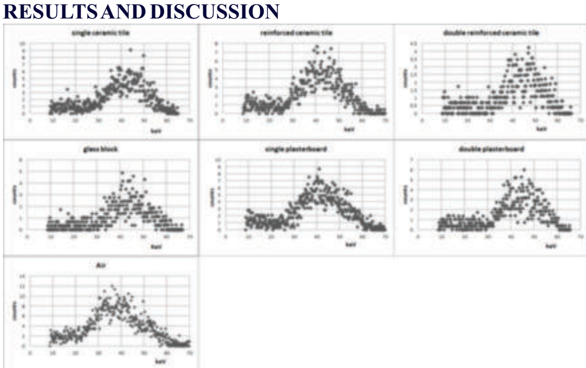

Figure 2. X-ray transmission spectra for Single ceramic tile, reinforced ceramic tile, double reinforced ceramic tile, glass block, single plasterboard, double plasterboard and without materials (air) for a field 16 cm x 2 cm2 are demonstrated, at 70 kVp X-ray tube voltage.

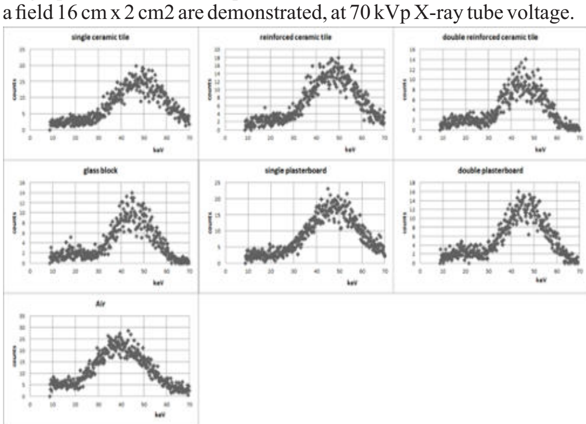

Figure 3. X-ray transmission spectra for: single ceramic tile, reinforced ceramic tile, double reinforced ceramic tile, glass block, single plasterboard, double plasterboard, and without materials (air) for a field 7.5 cm x 7.5 cm2 are demonstrated, at 70 kVp X-ray tube voltage.

In Figure 2 the measured X-ray transmission spectra for the materials: a) Single ceramic tile, b) reinforced ceramic tile, c) double reinforced ceramic tile, d) glass block, e) single plasterboard and f) double plasterboard for the X-ray field 16 cm x 2 cm is demonstrated, at 70 kVp X-ray tube voltage. In addition, in Figure 3, the corresponding measured X-ray transmission spectra for the X-ray field dimension of 7.5 cm x 7.5 cm is also demonstrated. Furthermore, the X-ray spectra of Single ceramic tile, double reinforced ceramic tile, single plasterboard and double plasterboard for the X-ray field dimension 16 cm x 2 cm at 70 kVp X-ray tube voltage, can also be found in the published literature [20]. In figures 2 and 3, the corresponding secondary X-ray spectra without a material present is also demonstrated. The average spectral energy calculated by equation 3 is demonstrated in Table 1. It can be observed that the 7.5 x 7.5 cm2 X-ray field systematically produces higher average X-ray energies than the 16 x 2 cm2 X-ray field. The above may be explained by the fact that the larger 7.5 cm x 7.5 cm field yields a higher number of secondary X-rays, which low energy component has a higher probability of reabsorption in the material due to the increased thickness (7.5 cm against 2 cm) they have to travel to exit the phantom. This can be also demonstrated by the secondary spectrum average energy (1st line in Table 1).

Table 1. Irradiation Filed 7.5 cm x 7.5 cm and 16 x 2 cm. Average Value Of Energy (keV) For 70 kVp X-ray Tube Voltage

	Irradiation filed 7.5 cm x 7.5 cm	**Irradiation filed 16 cm x 2 cm**
	Average energy (keV)	Average energy (keV)
Without material	39.57	37.31
Single plasterboard	45.87	40.09
Single ceramic tile	45.86	39.63
Reinforced in thickness ceramic tile	45.34	39.85
Double plasterboard	43.00	41.54
Double reinforced in thickness ceramic tile	42.39	41.58
Glass block	42.13	41.45

In Table 2 and Table 3, the secondary radiation dose rate for X-ray tube voltage 70 kVp for materials (a) to (f) and X-ray tube fields of 7.5 cm x 7.5 cm and 16 cm x 2 cm respectively, are presented. In the same Tables, the corresponding percent X-ray transmission for each material calculated by equation 4 is also presented. It may be seen that the smaller transmission, thus better radiation protection, is demonstrated by the commercially available glass block, while the single plasterboard demonstrates the larger. By comparing our calculated practical transmissions with transmissions presented in the literature, it can be observed that other building materials [5], except glass block, the materials examined in this work may produce similar attenuation properties with (i) PanelCrete of thickness less than 2cm, (ii) Aquapanel and Betopan of thickness less than 3cm and (iii) Gypsoplak superboard of thickness less than 4cm, as they have theoretically determined [5,6].

Table 2. Irradiation Filed 7.5 cm x 7.5 cm. kV, mA, ms. Secondary Radiation Dose Rate Measured For All Materials. With All Materials, With Stable Tube Voltage 70 kVp, tube current 10 mA, irradiation time 2000 ms.

	Secondary radiation dose rate	**Transmission %**
Without material	0.9 (mSv/hr)	-
Glass block	100.8 (μSv/hr)	11.2
Double reinforced in thickness ceramic tile	200.4 (μSv/hr)	22.2
Double plasterboard	200.5 (μSv/hr)	22.2
Reinforced in thickness ceramic tile	300.4 (μSv/hr)	33.3
Single ceramic tile	300.5 (μSv/hr)	33.3
Single plasterboard	400.4 (μSv/hr)	44.4

Table 3. Irradiation filed 16 cm x 2 cm. With all materials, with stable tube voltage 70 kVp, tube current 10 mA, irradiation time 2000 ms.

	Secondary Radiation Dose Rate	**Transmission %**
Without material	0.5 (mSv/hr)	-
Glass block	100.0 (μSv/hr)	20.0
Double plasterboard	150.0 (μSv/hr)	30.0
Double reinforced in thickness ceramic tile	150.0 (μSv/hr)	30.0
Reinforced in thickness ceramic tile	200.3 (μSv/hr)	40.0
Single ceramic tile	200.4 (μSv/hr)	40.1
Single plasterboard	300.0 (μSv/hr)	60.0

In Table 4, the practical TVL, as well as the corresponding number of TVLs, is also presented for 70 kVp X-ray tube voltage and both irradiation fields. It is seen that the smaller TVL value, is shown by a single ceramic tile and a larger glass block in both exposure fields, which denotes the higher efficiency of radiation absorption by the single ceramic tile. The higher absorption of the glass block shown in Tables 3 and 4, is due to its higher thickness, 7.9 cm compared to 0.7 cm of single ceramic tile.

Table 4. TVL Calculation For Materials (a) To (f) For 70 kVp X-ray Tube Voltage.

X-ray tube field 7.5cm x 7.5cm	**Measured thickness.**	**TVL (cm)**	**N_{TVL}**
single ceramic tile	0.7 cm	1.4	0,48
reinforced ceramic tile	0.8 cm	1.7	0,48
double reinforced ceramic tile	1.8 cm	2.7	0,65
glass block	7.9 cm	8.3	0,95
single plasterboard	1.3 cm	3.7	0,35
double plasterboard	2.6 cm	4.0	0,65
X-ray tube field 16cm x 2cm			
single ceramic tile	0.7 cm	1.8	0,39
reinforced ceramic tile	0.8 cm	2.0	0,39
double reinforced ceramic tile	1.8 cm	3.5	0,52
glass block	7.9 cm	11.4	0,69
single plasterboard	1.3 cm	6.0	0,22
double plasterboard	2.6 cm	5.0	0,52

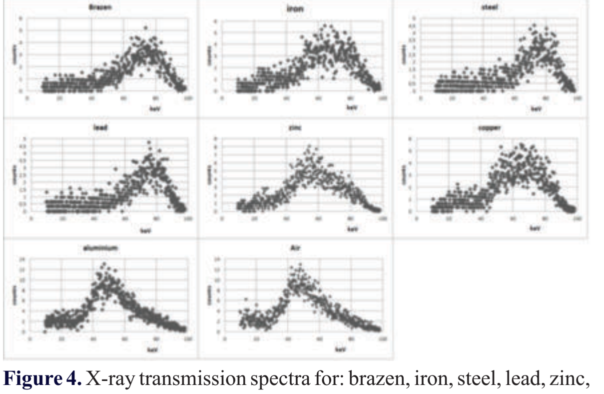

Figure 4. X-ray transmission spectra for: brazen, iron, steel, lead, zinc, copper, aluminium and without materials (air) for a field 40 cm x 40 cm2 are demonstrated, at 100 kVp X-ray tube voltage.

In Figure 4, the measured X-ray spectra for brazen with thickness at 1.0 mm, iron with thickness at 1.0 mm, steel with thickness at 1.0 mm, lead with thickness at 1.0 mm, zinc with thickness at 1.0 mm, copper with thickness at 1.0 mm and aluminium with thickness at 2.0 cm are presented. In Table 5, their corresponding average energy values are shown. A calculation of the X-ray transmittance for this energy is not presented since current literature strongly suggests lead as a very effective material for all applications [3,4,7,8]. The above can intuitively be demonstrated by inspecting the peak count values measured by the spectrometer after lead and compare it with the other high Z materials.

Table 5. Average Value Of Energy (keV) Of All Materials. Irradiation Filed 40.0 cm x 40.0 cm for X-ray Tube Voltage 100kVp

	Irradiation filed 40.0 cm x 40.0 cm
	Average value of energy
Without material	50.10
Brazen	62.00
Iron	61.00
Steel	65.60
Lead	67.00

Mercury	56.00
Copper	58.50
Aluminum	51.37

In Table 6 and Table 7, the X-ray mapping performed for fields of 7.5 cm x 7.5 cm and 16 cm x 2 cm at 70 kVp X-ray tube voltage is also demonstrated.

Table 6. Secondary Dose For An Irradiation Field Of 7.5 cm x 7.5 cm, Tube Voltage 70kVp, 32 mAs And 2.9 ms Exposure Time.

Angle of scattered radiation (degrees)	0°	45°	90°	135°	180°	225°	270°	315°
Distance from the phantom (m)	Secondary radiation dose rate (μGy)							
0.5	0.548	0.495	0.500	0.628	0.589	0.748	0.857	0.730
1.0	0.143	0.130	0.140	0.151	0.139	0.156	0.174	0.161
1.5	0.097	0.055	0.085	0.080	0.073	0.079	0.085	0.073

Table 7. Secondary Dose For An Irradiation Field 16 cm x 2 cm Tube Voltage 70kVp, 32 mAs And 2.9 ms Exposure Time.

Angle of scattered radiation (degrees)	0°	45°	90°	135°	180°	225°	270°	315°
Distance from the phantom (m)	Secondary radiation dose rate (μGy)							
0.5	0.384	0.435	0.383	0.462	0.450	0.507	0.563	0.546
1.0	0.098	0.118	0.108	0.130	0.094	0.101	0.092	0.121
1.5	0.074	0.046	0.062	0.058	0.049	0.055	0.042	0.047

It can be seen that the higher measured dose is at 270o degrees at 0.5 cm distance from the phantom. In each case, at 1.5 cm distance from the phantom, the measured dose falls. It is interesting to notice however, that at 1.5 cm the measured value of 270o falls to about 10% of its 0.5 m value. The higher scatter at 1.5 m in both irradiation fields is at 0o, 90o and 270o. In the first two angles, the measured values are over 16% of the 0.5 m value. Higher scatter components for the 90o degrees angle has been reported in the literature, but at different geometry conditions [23].

CONCLUSION

In this paper, the exposure and spectral characteristics of scatter radiation passing through shielding materials were examined. It was found that under 70 kVp conditions, the glass block mainly due to its thickness provided the best radioprotection barrier.

REFERENCES

1. Council Directive 2013/59/EURATOM on 5 December 2013 “laying down basic safety standards for protection against the dangers arising from exposure to ionising radiation, and repealing Directives 89/618/Euratom, 90/641/Euratom, 96/29/Euratom, 97/43/Euratom and 2003/122/Euratom”.
2. IAEA Safety Standards “Radiation Protection and Safety of Radiation Sources:International Basic Safety Standards, General Safety Requirements Part 3”, Printed by the IAEA in Austria July 2014 STI/PUB/1578.
3. B.R. Archer, T.R. Fewel, B.J. Conway, and P.W. Quin:“Attenuation properties of diagnostic x-ray shielding materials” Medical Physics 21, 1499-1507, 1994
4. I.A. Tsalafoutas, E. Yiakoumakis, A. Manetou and A. Flioni-Vyza “The diagnostic X-ray protection characteristics of YTONG, an aerated concrete based building material” The British Journal of Radiology, 71, 944-949, 1998.
5. I.A. Tsalafoutas, E. Yiakoumakis, P. Sandilos, L. Vlachos and Ch. Proukakis “The diagnostic X-ray protection characteristics of Panelcrete, Aquapanel, Betopan and Gypsoplack Superboard” The British Journal of Radiology, 74, 351-357, 2001.
6. I.A. Tsalafoutas, E. Yiakoumakis and P. Sandilos “A model for calculating shielding requirements in diagnostic X-ray facilities” The British Journal of Radiology, https://doi.org/10.1259/bjr/21741358
7. M. Petrantonaki, C. Kappas, E. Efstathopoulos, Y. Theodorakos, and G."Calculating shielding requirements in diagnostic X-ray departments." The British journal of radiology. 72. 179-85, 1999.
8. NCRP 147 “Structural Shielding design for medical X-ray imaging facilities” Recommendations of the National Council on Radiation Protection and Measurements, 2005.
9. W.Tc.C. Wolvekamp "Basic Principles of Thoracic Radiography", https://doi.org/ 10.1080/01652176.1995.9694580
10. M. Bochman, E. Ludewig, M-E. Krautwald-Junghanns, M. Pees "Comparison of the image quality of a high resolution screen-film system and a digital flat panel detector system in avian radiography" Veterinary Radiology & Ultrasound, 52, 256–261, 2011.
11. N. Ackerman, C.P. Spencer, D.A. Hager, P.W. Poulos "Radiation Exposure During Equine Radiography" Veterinary Radiology, 29, 198-201, 1988
12. European Commission Radiation Protection 136 “European Guidelines on Radiation Protection in Dental Radiology. The safe use of radiographs in dental practise” Directorate-General for Energy and Transport, Directorate H — Nuclear Safety and Safeguards, Unit H.4 — Radiation Protection, 2004.
13. V. Tsapaki “Radiation protection in dental radiology-Recent advances and future directions”, Physica Medica, 44, 222-226, 2017.
14. Santos, Marcus Aurelio P. dos, Marcus, Fragoso, Maria da Conceicao F, Lima, Ricardo de A, Hazin, Clovis A., & Moralles, Mauricio (2010). Dental x-ray spectrometry with cadmium telluride detectors. International Atomic Energy Agency (IAEA): https://inis.iaea.org/search/search.aspx?orig_q=RN:42072461 (last accessed April 2022).
15. Spyropoulos B., Manousaridis G., Papathymiou A. (2009) A high-resolution Schottky CdTe detector based spectrometric determination method of the kilovoltage applied to dental X-ray tubes. In: Vander Sloten J., Verdonck P., Nyssen M., Haueisen J. (eds) 4th European Conference of the International Federation for Medical and Biological Engineering. IFMBE Proceedings, vol 22. Springer, Berlin, Heidelberg https://doi.org/10.1007/978-3-540-89208-3_351
16. R. Pauwels, H. Stamatakis, G. Manousaridis, A. Walker, K. Michielsen, H. Bossmans, R. Bogaerts, R. Jacobs, K. Horner, K. Tsiklakis "Development and applicability of a quality control phantom for dental cone-beam CT" Journal of Applied Clinical Medical Physics, 12, 245-260, 2011.
17. G. Manousaridis, C. Koukorava, C. J. Hourdakis, V. Kamenopoulou, E. Yakoumakis and K. Tsiklakis "Establishment of Diagnostic Reference Levels for Dental Intraoral Radiography" Radiation Protection Dosimetry, 156, 455-457, 2013
18. G. Manousaridis, C. Koukorava, C. J. Hourdakis, V. Kamenopoulou, E. Yakoumakis and K. Tsiklakis "Establishment of Diagnostic Reference Levels for Dental Panoramic Radiography in Greece" Radiation Protection Dosimetry, 165, 111-114, 2015.
19. A. Nemtoi, C. Czink, D. Haba and A. Gahleitner “Cone beam CT: a current overview of devices” Dentomaxillofacial Radiology, 42, 20120443, 2013
20. I. Vlachos, X. Tsantilas, G. Fountos, H. Delis, I. Kandarakis and G. Panayiotakis "Effect of Common building materials in narrow shaped X-ray fields transmission" Journal of Physics: Conference Series 637, 012034, 2015
21. I. Vlachos Doctorate Dissertation "Spectroscopy and Dosimetry of Secondary Radiation for Radiology Systems", University of Patras, 2016, http://hdl.handle.net/10442/hedi/37053, (last accessed April 2022)
22. G. McVey, and H. Weatherburn “A study of scatter in diagnostic X-ray rooms” The British Journal of Radiology, 77, 28-38, 2004
23. I. Vlachos, X. Tsantilas, N. Kalyvas, H. Delis, I. Kandarakis and G. Panayiotakis "Measuring Scatter Radiation in Diagnostic X-rays for Radiation Protection Measurements" Radiation Protection Dosimetry, 1-4, 2015, doi:10.1093/rpd/ncv093.
24. K. Noto, K. Koshida, H. Iida, T. Yamamoto, I. Kobayashi, C. Kawabata. “Investigation of scatter fractions for estimating leakage dose in medical X-ray imaging facilities”. Radiol. Phys. Technol., 2, 138-144 (2009).
25. M. Krmar, N.Bucalovic, M.Baucal, N.Jovancevic "Possible use of CdTe detectors in kVp monitoring of diagnostic X-ray tubes", Nuclear Instruments and Methods in Physics Research A, 622, 256-260, 2010.
26. N. Martini, V. Koukou, C. Michail, P. Sotiropoulou, N. Kalyvas, I. Kandarakis, G. Nikiforidis, and G. Fountos "Pencil Beam Spectral Measurements of Ce, Ho, Yb, and Ba Powders for Potential Use in Medical Applications" Journal of Spectroscopy, Article ID 563763, 2015, http://dx.doi.org/10.1155/2015/563763
27. See http://www.amptek.com/ (April 2022, date last accessed).
28. See http://www.flukebiomedical.com/ (April 2022, date last accessed).
29. Fluke Biomedical model 451P-DE-SI. https://www.flukebiomedical.com/sites/ default/files/resources/451P-DE-SL_ENG_A_W.PDF (April 2022, date last accessed).
30. See https://www.alatuji.com/images/products/files/radiasi.pdf (April 2022, date last accessed).